MATHEMATICAL BIOSCIENCES
AND ENGINEERING
Volume **10**, Number **3**, June **2013**

doi:10.3934/mbe.2013.10.523

pp. **523–550**

DIFFUSION RATE DETERMINES BALANCE BETWEEN EXTINCTION AND PROLIFERATION IN BIRTH-DEATH PROCESSES

Hilla Behar, Alexandra Agranovich
and Yoram Louzoun

Department of Mathematics
Bar Ilan University
Ramat Gan, Israel

Abstract. We here study spatially extended catalyst induced growth processes. This type of process exists in multiple domains of biology, ranging from ecology (nutrients and growth), through immunology (antigens and lymphocytes) to molecular biology (signaling molecules initiating signaling cascades). Such systems often exhibit an extinction-proliferation transition, where varying some parameters can lead to either extinction or survival of the reactants.

When the stochasticity of the reactions, the presence of discrete reactants and their spatial distribution is incorporated into the analysis, a non-uniform reactant distribution emerges, even when all parameters are uniform in space.

Using a combination of Monte Carlo simulation and percolation theory based estimations; the asymptotic behavior of such systems is studied. In all studied cases, it turns out that the overall survival of the reactant population in the long run is based on the size and shape of the reactant aggregates, their distribution in space and the reactant diffusion rate. We here show that for a large class of models, the reactant density is maximal at intermediate diffusion rates and low or zero at either very high or very low diffusion rates. We give multiple examples of such system and provide a generic explanation for this behavior. The set of models presented here provides a new insight on the population dynamics in chemical, biological and ecological systems.

1. **Introduction.** Most biological processes involve the autocatalytic proliferation of individual agents. The basic mathematical modeling of these phenomena was carried out 200 years ago in the context of population growth [54,76]. The combined, Malthus-Verhulst equation is known nowadays as the logistic equation that describes the logistic growth [42]. In its simplest interpretation it describes the evolution of population, say, a bacteria colony on a Petri dish. Similar dynamics dictates the spread of a favored gene, of new species [74], of a disease that is distributed via infection [39]and of almost any other autocatalytic process.

Since the pioneering works of Fisher [20] and KPP [41], the dynamics of the logistic growth processes on spatially extended domains has attracted a lot of interest. Typically, the spatial dynamics of individual agents has been assumed to be diffusive, leading to a partial differential reaction-diffusion equation that involves both logistic growth and diffusion on spatial domain. The most prominent feature of this Fisher (or FKPP) equation is the appearance of a soliton solution, the Fisher front,

2010 *Mathematics Subject Classification.* Primary: 58F15, 58F17; Secondary: 53C35.
Key words and phrases. AB model, adaption, logistic growth, directed percolation, localization.

with a typical width and velocity. The steady state of the system, however, is the same as the steady state of the logistic growth on a single patch, since the domain is considered as homogenous, with uniform proliferation coefficient and carrying capacity.

In recent years, many works have dealt with the statics and dynamics of the logistic growth on spatially heterogeneous domains or under fluctuating environmental conditions. The interest in such phenomena ranges from out of equilibrium statistical mechanics [28, 35, 58], to chemistry [23, 64] and biology [27, 45, 49, 57, 62]. These theoretical works led to experimental biological validations of the expected dynamics in bacterial populations [45]. An interesting problem manifested in the application of the Malthus-Verhulst equation to biological systems is the discrete nature of the reactants. The deterministic ordinary (or partial) differential equations used to model systems of individual agents fail to capture the effect of the intrinsic noise associated with the stochastic behavior of individual reactants.

Assume a population with a birth rate twice larger than the death rate. In such a case, the logistic growth equation predicts that the empty state is unstable and the population grows until it saturates. However, suppose that the system may support only, say, three reactants. If the stochastic character of the death and birth processes is taken into account, there is finite probability per unit time for all three reactants to die without any birth. In such a case the system is trapped in its frozen absorbing state. This is a common feature of many individual reactants systems the extinction of any finite population (say, a single colony) due to large stochastic fluctuations that drive the system into the absorbing state. This example is by no means unique: as autocatalysis involves exponential growth, the system is very sensitive to stochastic fluctuations, both of the population itself and of the environment. In order to take these effects into account, one should consider the Masters equation (Forward Kolmogorov Equation) that describes the actual stochastic process, and to regard the deterministic reaction-diffusion equation as some sort of mean field approximation, perhaps with appropriate corrections. Alternatively, the results of numerical simulation may be used in order to identify the regime of validity of the mean field deterministic equations and to determine the system behavior beyond these limits.

The main goal of the current review is to show that the balance between regions in such an absorbing state and regions in a growing phase leads to a dynamic non-uniform spatial distribution of reactants. This distribution can be related to multiple types of previously studied dynamic systems. The most interesting one is directed percolation (DP) [11] in the d+1 space-time. DP assumes a lattice based dynamical process, where each lattice point can be either active (full) or inactive (empty), with constant birth, death and diffusion probabilities. The system dynamics are represented through the presence or absence of unidirectional edges between neighboring spatial position from time t to the time t+1. The probability for the existence of such an edge is denoted the filling fraction. In finite dimensions ($2 < d < \infty$), DP systems show a second order phase transition at a critical filling fraction. Below this density, after a long enough time, the system will be empty, while above it will contain active sites. The DP represents a universality class by itself. Grassberger and Janssen [25, 34] proposed that under a set of limiting conditions, most dynamical systems belong to the DP universality class.

We here study four different scenarios, ranging from simple expanding populations to predator prey systems to show that a similar principle may explain features in all the different systems:

1. At low diffusion rates, every position collapses to the abosribing state, since the carrying capacity is always finite, and the reactant population is extinct.
2. At very high diffusion rates, the system behaves like the ODE approximation. If the ODE approximation converges to 0, so does the simulation.
3. At intermediate range of diffusions, a very high reactant density appears which is due to an adaptation of the reactants to random fluctuations in the catalyst density.

All the models studied here are based on the following common model:

2. **Common model.** Consider a system of catalysts and reactants, both are discrete agents that wander around diffusively on a d-dimensional lattice. The main feature of the model is catalysts induced growth, namely, the reactants multiplicate autocatalytically in the presence of catalysts. In previous works, the linearized version of logistic growth in the presence of wandering catalysts has been considered. This model was named the AB model [49–53, 73]. This simple model contains a diffusive catalysts A, and a diffusive, proliferating and dying reactants B. Reactant proliferation occurs only in the presence of the catalyst (A), and it occurs with a rate of β_B. Reactant death occurs spontaneously with a constant rate of δ_B. These reactions can be summarized by:

$$A + B \xrightarrow{\beta_B} A + B + B \tag{1}$$

$$B \xrightarrow{\delta_B} \emptyset$$

The diffusion rates are D_A andD_B for the catalyst A and reactant B respectively. As the catalysts A are eternal objects, their total number is time independent. The catalyst density per unit volume is denoted by N_A. It was shown that, in spite of this system seeming simplicity, it induces complex dynamics. At the mean field level, the diffusion of the catalysts implies a uniform distribution. Accordingly, the growth rate at each spatial location is given by $\beta_B N_A - \delta_B$. If this quantity is positive the system proliferates and if it is negative the system is driven to extinction. When the stochastic motion of the A-s and the Poisson fluctuations in the growth rate are taken into account, the situation is different. It turns out that even if on average the system is in its extinction phase, there are still spatial patches of positive growth rate ("oases") due to the fluctuations associated with the catalyst discrete nature. Within each oasis there is an exponential proliferation of the B reactants, and localized colonies of B emerge around these oases. Once such a colony proliferates, its spatial size grows linearly in time, and the diffusive motion of the catalysts is not fast enough to "escape" from the colony. Thus, the B reactants "adapt" to the fluctuating environment, leading to a proliferating phase well below the "mean field" extinction transition, i.e., even if $\beta_B N_A - \delta_B \ll 0$ [52, 72, 73].

The basic difference between the classical AB model and its PDE counterpart is the emergence of localized structures that induce B reactant population growth. We will show that such structures emerge in the presence of a limited A lifespan (a "massive" A in field theory terms) and in the presence of B competition, but that in contradiction with the original AB model, there is a phase transition between the localized surviving and uniform decaying states even in two dimensions.

We here study four systems that are different extensions of this basic model in very different domains, and show that they all have a maximal reactant density at intermediate diffusion rates. These systems will be analyzed using the following methods:

3. Methods.

3.1. ODE numerical solution.

When studying the behavior of the system that does not take into account possible spatial in-homogeneities, or the possible discrete aspect of the interactions, we use a numerical ODE solver. The ODEs studied here are non-stiff in the parameter regime studied, and was solved numerically using the ode45 Matlab function, based on an explicit fourth order Runge-Kutta formalism [6].

3.2. PDE numerical solution.

In order to examine the influence of the spatial distribution of the reactants, we use a PDE solver. The solver uses a first order spatial diffusion scheme and a fourth order Runge-Kutta formalism for the time derivatives. Note that the PDE solver does not take into account stochastic fluctuation in the system.

3.3. Simulations.

The stochastic models are studied using Monte-Carlo simulations. These simulations have been performed on a d-dimensional lattice (Z^d). The simulations include diffusion between the cells and stochastic fluctuations. These fluctuations originate from the fact that the reactions in the simulation are treated as independent random events and that each lattice site has a discrete number of agents (and not a continuous number as in the ODE and the PDE).

The precise description of the simulation can be found in previous publications [3, 52, 73]. In the absence of diffusion, the simulation results can be treated as an ensemble of zero dimensional systems. The average of this ensemble is the averaged zero dimensional stochastic counterpart of the mean field results.

3.4. Single colony analysis for the directed percolation.

In order to study the survival condition of localized reactant aggregates (also denoted as islands) around an "oasis", i.e., spatio temporal catalyst concentration is analyzed, we assume a constant number of catalysts at the center of a reactant aggregate, and calculate the shape of the reactant aggregate using standard partial differential equations. We find the minimal aggregate size requested for the system survival assuming a low catalyst diffusion rate and a low catalyst density. A Directed Percolation analysis is then used to estimate the survival probability of the whole system, given the probability that the aggregate surrounding an oasis will "touch" another aggregate by the time the oasis is dissolved, as a function of its volume fraction. The approximation here is to neglect the diffusive correlation of catalyst fluctuations beyond some typical time scale.

3.5. Directed percolation analysis.

Directed percolation [11] is a model for the spreading of a substance in a lattice in discrete time steps. Each lattice point can have a value of zero or one, and lattice points with values of one can invade a neighboring point. The fraction of lattice points with values of one is determined by the ratio between the invasion probability and the extinction probability at each site. If this value is higher than a percolation threshold, the lattice occupancy (the fraction of lattice points that have a value of one) will be positive at finite times, while below this value, it will be null. The transition between two states is a second order phase transition [31]. In the current analysis, the value at a given lattice point

was computed based on its own value, and the values of its first neighbors in the previous step (2 in 1D, 4 in 2D and 6 in 3D simulations). First, a disappearance probability $p(div) = p : 1 \to 0$ was applied to each lattice point with a value of 1. Then a probability of diffusion $p(inv) = p : 0 \to 1$ was applied from each lattice point that had a value of 1 in the previous time step to its nearest neighbors.

4. **Model 1 - Dying catalysts.**

4.1. **Model description.** In the AB model described above, the catalysts were eternal [3]. Replacing them by dying catalysts alters the dynamics. As in the common model, the system contents two kinds of agents: catalysts A and reactants B, both of which are spreading randomly with diffusion rates $D_A$and $D_B$correspondingly on a lattice Z^d. The catalysts A are introduced into the system with a constant rate of $\beta_A$and die with a rate of δ_A. The dynamics of the B reactants is similar to the one used in the AB model. Thus, the dying A reactant system contains the following reactions:

- $A + B \to A + B + B$ with a rate of β_B.
- $B \to \emptyset$ with a rate of δ_B.
- $A \to \emptyset$ with a rate of δ_A.
- $\emptyset \to A$ with a rate of β_A.
- A and B diffuse at rates of D_A and D_B.

The mean-field, deterministic, rate equations describing this system are:

$$\frac{\partial N_A}{\partial t} = D_A \nabla^2 N_A - \delta_A N_A + \beta_A \tag{2}$$

$$\frac{\partial N_B}{\partial t} = D_B \nabla^2 N_B - \delta_B N_B + \beta_B N_A N_B$$

where $N_A$and N_B are the densities of the catalyst and the reactant, respectively. After a long enough time (much longer than $\frac{1}{7}\delta_A$), the A particles density is $\langle N_A \rangle = \frac{\delta_A}{\beta_A}$. The effective growth rate of the reactants becomes $\beta_B \langle N_A \rangle - \delta_B$. The extinction transition is expected to occur at $\beta_B \frac{\delta_A}{\beta_A} = \delta_B$. Basically, the fact that reactants multiplication occurs at close proximity with the catalyst may lead to deviations from this prediction since the immediate environment seen by the B population is less hostile than the average environment. This may lead to a living system even below the mean field extinction transition. Our first step is to check this hypothesis numerically.

4.2. **Numerical simulations.** We have simulated the dying catalysts system using the following parameters $\delta_A = 1, \delta_B = 1, D_A = 0, D_B = 0.25$and varied β_A. We checked at what values of $\frac{\delta_A}{\beta_A} = \frac{1}{N_A}$and $\beta_B$the survival extinction transition occurs (Figure 1). One can clearly see that the survival threshold is much below the one expected in the mean field analysis, in correspondence with the adaptation behavior demonstrated in the AB model. Moreover, it seems from the figure that, in a wide region of the parameter space, the transition line depends very weakly on the average $\frac{\delta_A}{\beta_A}$, in stark qualitative contrast with the mean field analysis.

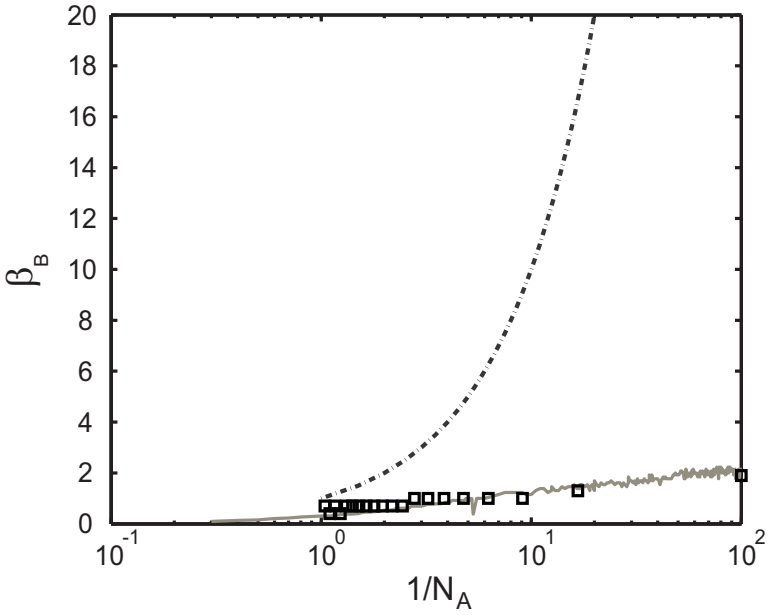

FIGURE 1. **Comparison between mean field, simulations and Directed Percolation for a system with dying catalysts.** The simulation was done with the following parameters: $\delta_A = 0.01, \delta_B = 1, D_A = 0, D_B = 1$.For these parameters, the values $\beta_A$and $\beta_B$were varied. The drawing represents the values of $\frac{1}{N_A} = \frac{\delta_A}{\beta_B}$and β_B for which the survival extinction transition occurs. One can clearly see that the survival threshold in the simulations (solid gray line) is much below the one expected in the mean field analysis (dashed dotted line) and very close to the one predicted by the DP (black boxes).

4.3. **Dying catalyst - directed percolation picture of the extinction transition.** In order to understand the difference between the numerical simulations and the ODE models, one must incorporate the discrete aspects of the catalysts. Given this discrete nature, every lattice site has a given number of catalysts. Assume for example that the average catalyst density would be 0.01. This would not mean that each lattice site would have 0.01 catalysts. Rather, 0.01 of the sites will have a catalyst (or more), while around 99 % of sites would have no catalysts. Around each catalyst a colony of reactants can grow for deviation of the shape of the colony [3].

As the lifespan of a reactant colony is finite, any single colony is bound to decay. The simple criteria for the survival of the reactants are that, by the time the catalysts disappear, the colony "touches" at least one other colony. If one disregards the spatial correlation between the catalysts (this correlation is related to the diffusive motion of the catalysts, and let us assume for the moment that the catalysts are standing still so there indeed is no such correlation), the picture is of d+1 dimensional space-time with finite, constant density of finite "length" (i.e., time span) catalyst columns (representing the catalyst aggregate in the center of the colonies) randomly distributed. Around each of these columns a "cone" (in space-time) of

reactants is developed, and the question of the reactants survival translates itself to the language of percolation theory, namely, whether or not the system is below or above the directed percolation threshold for cones.

Now let us plug in the parameters. First, the directed percolation threshold for a system of cones in 2+1 dimensions has been found numerically to be $p_c = 0.75$ (see Figure 2). The probability to find m catalysts at a single lattice point is given by the Poisson distribution:

$$P_{m=}\frac{\left(\frac{\beta_A}{\delta_A}\right)^m \cdot e^{-\frac{\beta_A}{\delta_A}}}{m!} \tag{3}$$

The system survives for a long time if the filling fraction is higher than the directed percolation transition threshold ($P_m > p_c$). The percolation threshold was computed for an island diameter of one and length of one, so that the island size must be rescaled to fit the percolation estimate

$$(\nu\tau_{mA})^d \tau_{mA} P_m > p_c \tag{4}$$

where $\tau_{mA} = \frac{1}{m(\delta_A + D_A)}$ is determined by the stochastic parameters. Both ν and p_c are dimensionally dependent, and all the quantities on the left hand side are m dependent. In other words for each value of m selected, a different threshold would be obtained. The system will survive if there exists at least one integer m such that this inequality holds. In Figures 1 and 3, the phase diagram extracted from this condition is compared with the numerical simulations. Clearly there is a good qualitative agreement.

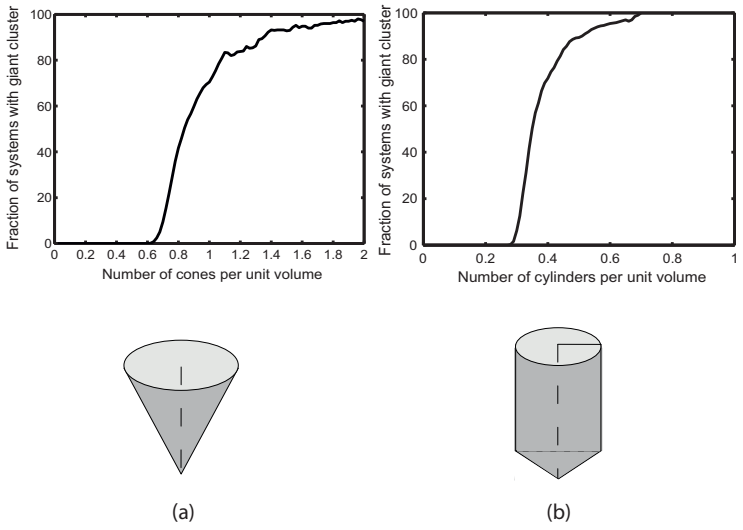

FIGURE 2. **DP analysis**. Islands shapes in the case of: (a) dying catalysts model; (b) competing reactants model. Difference in the percolation thresholds as a result of difference in the shapes of islands in space time in the two first models studied here.

Thus, to summarize this first model, the dynamics of such a system is determined by limited regions of finite population surrounded by large empty regions. The dynamics is governed by the balance between the extinction of these regions and the invasion of new catalyst rich regions. Thus, three regimes can be defined in this model:

- At low diffusion values, the reactant density goes to 0, since local aggregates do not connect one to each other.
- At high diffusion values, the reactant density goes to 0, like the ODE approximation
- At intermediate values, there is a non-zero reactant density, which eventually diverges.

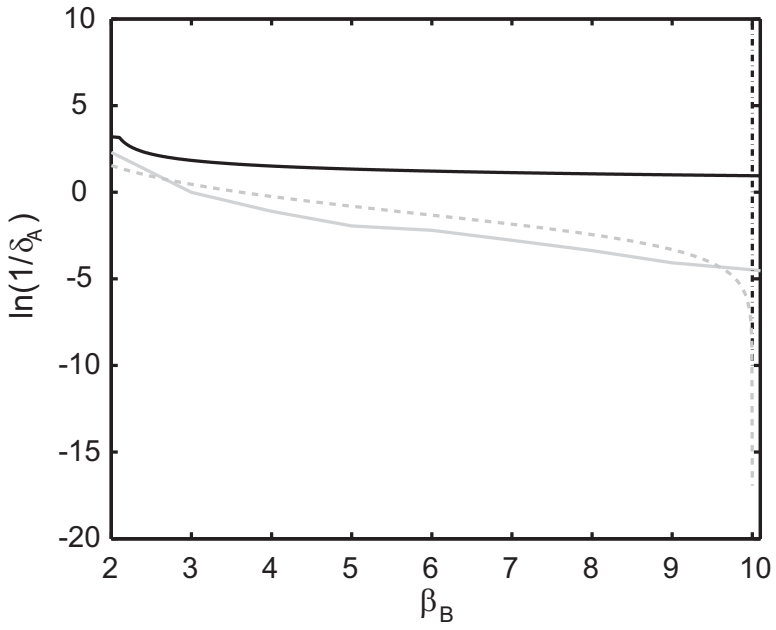

FIGURE 3. **Comparison between mean field, simulations, field theory and Directed Percolation for a system with dying catalysts**. The phase transition is depicted here as a value of $\ln(1/\delta_A)$ for β_B each value. The mean field prediction is that the system would survive only for $\beta_B > 10$, independent of $\ln(1/\delta_A)$ (since the value of β_A/δ_A is fixed). The simulation (full gray line), the perturbative results (dashed black line) and the DP (full black line), on the other hand, all predict survival for much lower values of β_B given that the value of δ_A is low enough. Note that the discrepancy between the DP and the simulations grows as the value of δ_A increases. This is the obvious result of the collapse of the DP assumption (i.e. a much faster B than A dynamics). At even higher values of δ_A, the simulation itself is not precise anymore since we cannot decrease the time step to allow a small number of A reactions to occur in a given time step. The parameters used in this figure are: $\langle N_A \rangle = 0.1, \delta_B = 1, D_A = 0, D_B = 1$.

5. Model 2 - Limited carrying capacity.

5.1. **System description.** While in the previous model a finite lifespan of the catalysts has been considered, another important characterization of birth death processes is the finite carrying capacity (per unit volume) of the system. The original AB model, as well as its dying catalyst extension, allows for two different phases of the whole system: in the extinction phase the number of reactants goes to zero, while in the proliferation phase this number goes to infinity. To be more realistic, we introduce a nonlinear saturation mechanism into the system. This limiting mechanisms is mainly related to the competition for common resources such as space, food, or water, and is the driving force of Darwinian Evolution (see [52]). The deterministic growth process is then generically described by the following coupled rate equations:

$$\frac{\partial N_A}{\partial t} = D_A \nabla^2 N_A \tag{5}$$

$$\frac{\partial N_B}{\partial t} = D_B \nabla^2 N_B - \delta_B N_B + \beta_B N_A N_B - \sigma_B N_B^2$$

These equations incorporate the features of the logistic growth into the catalyst induced proliferation mechanism. There are many microscopic processes that yield, upon cross-graining, the $-\sigma_B N_B^2$ term, such as mutual annihilation $B + B \to \emptyset$ or destruction of one B reactant by the other: $B + B \to B$. It is known, however, that for these processes in a homogenous environment (uniform birth-death rate at each site), there is a difference between the predictions of the mean-field equations and the behavior of the real, stochastic process. We have here used a competition term represented by the death of a reactant when two reactants meet.

The model considered contains the following processes:

- An immortal diffusing catalyst with the a rate of D_A.
- A reactant B proliferating in the presence of an A catalyst, dying, diffusing and competing with other reactants with rates of β_B, δ_B, D_B and σ respectively. The competition here means that when two B reactants meet, one of them will die with probability σ_B.

5.2. **Survival of system with competition - directed percolation.** The directed percolation argument may also be used here, with the lifespan of a m A-s aggregate taken as $\frac{1}{mD_A}$. As long as the competition term effect is negligible, the B islands grow linearly as in the previous case. In this case, we would use the DP threshold obtained for cones. Once the competition at the center of the island becomes important, the islands size stabilizes. In space time, this produces a cone converging into a cylinder. If the islands survive for a long time, we can ignore the cones and assume space is filled with cylinders.

The scaled DP estimate in the case when the islands are disrupted before they stabilize is as before:

$$\left(\nu\left(\tau_{mA}\right)\tau_{mA}\right)^d \tau_{mA} P_m > p_c(cone) = 0.75 \tag{6}$$

where P_m is the frequency of m A catalysts aggregates, τ_{mA} is the average existence time of such aggregates, and $\nu\left(\tau_{mA}\right)$ is the B colony radius at time τ_{mA}. On the other hand, if the colonies are stabilized for a long time before they disappear, the system survival condition is:

$$r(\infty)^d \tau_{mA} P_m > p_c(cylinder) = 0.34 \tag{7}$$

where we have replaced $r(\tau_{mA})$ by $r(\infty)$. Note that although $p_c(cylinder) < p_c(cone)$, $r(\tau_{mA}) \ll \nu(\tau_{mA})\tau_{mA}$ and the survival condition (7) is worse than (6). We have previously developed an analytical estimate for the time-space structure of reactant aggregates, and compared the percolation results using such shapes with the full simulation [3].

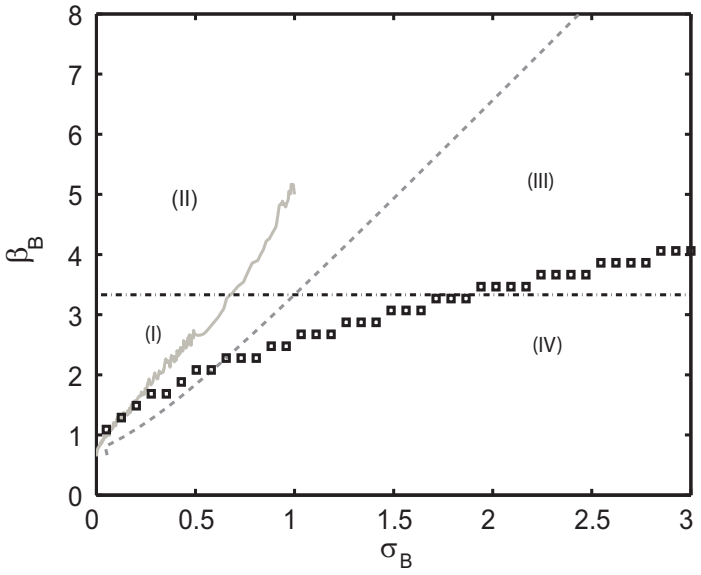

FIGURE 4. **Competing B-agents**. Comparison between the results of the DP, FT, simulations and mean field. The dashed doted line is the mean field, the DP is in red squares, the FT is the dashed line and the results of the simulations are presented as a solid line. Regions (I) and (II) are the survival regions according to the simulations, while the mean field estimate predicts survival in regions (II) and (III). Region (IV) is the part of phase space where both simulations and the mean field predicts the extinction of all B agents. The places where the both estimates overlap are obviously regions (II) and (IV). An interesting phenomena observed in zone (III) is that the islands are destroyed because of large competition rate and there is no continuous (infinite) B mass near the source A. Thus one cannot assume anymore a continuous B agent persistence at each location. Note that the DP analysis is precise at low $\beta_B$and σ_B. The parameters used for this figure are $N_A = 0.3, \delta_B = 1, D_B = 0.1, D_A = 0.1$.

The results of numerical simulations for the competing reactant case are presented in Figure 4 with the parameters $\delta_B = 1, D_A = D_B = 0.1, \langle N_A \rangle = 0.3$ and varying values of σ_B and β_B. According to the mean field theory the extinction transition should take place at$\beta_B = 3.33$,independent of the nonlinear interaction

σ_B. One can see that this is not the case. In fact, for small σ_B the transition is shifted downward, as in the AB model, due to adaptation of the reactant colonies to the fluctuating environment, while for large σ_B the opposite process, extinction of colonies attributed to the stochastic fluctuations in the number of B-s, dominate and the transition point is shifted upward.

To summarize, the dynamics of this system are completely equivalent to the first presented model, with the main difference being that here at intermediate diffusion rates, the reactant concentration is finite, while in the previous one, it diverged.

6. **Model 3 - Lotka Voltera system.**

6.1. **Description of the model.** In the early 1920's, Lotka and Voltera have shown that a system containing the negative feedback of a predator on a prey can lead to sustained oscillations [46–48,77]. This observation as expressed through the now classical Lotka Voltera (LV) predator-prey (PP) equations has been extensively studied. The original LV model has been enlarged to include more complex interaction terms [5,9,19,22,24,32,57,61,66], spatial heterogeneity [14,19,21,60,61,79] (for a review see [10]) and stochastic interactions [13,16,17,37,43,44,55,56,78]. In discrete stochastic models, the LV model also has absorbing states of zero predator and prey or zero predator and either finite or infinite prey populations. In a deterministic continuous system, either the fixed point equivalent of the stochastic absorbing state is unstable and then each trajectory that leaves it reaches the stable fixed point; or it is stable and small perturbations exponentially decrease.

Thus apparently, the LV is very different from the dynamical models studied up to now. We here show that LV models can show similar transitions to what has been discussed in the two previous models.

An example of that would be an abstraction of the lymphocyte-pathogen dynamics. Lymphocytes have a pathogen independent basal production rate in the bone marrow or in the thymus [1], and basal division and death rates. Upon infection, a few clones of pathogen specific lymphocytes grow and destroy the pathogen, until the pathogen is eventually eradicated, within days to weeks [33]. Once the pathogen disappears, the lymphocyte clones size decays. The decay can either be to the basal level, or to a slightly higher level, if memory cells are formed [7,12,38,63,69]. These interactions can be summarized by the following reactions:

- proliferation of the pathogen x with a rate of α;
- duplication of host lymphocytes in response to an encounter with a pathogen with a rate of ν;
- pathogen destruction by the host lymphocytes with a rate of γ;
- creation of new lymphocytes in the hosts bone marrow/thymus with a rate of λ;
- lymphocytes natural death with a rate of σ.

Lymphocytes and pathogens obviously do not move in an empty space. Instead they travel through the blood and the lymphatic system, but for the sake of simplicity, we here describe the lymphocytes and pathogen movement as diffusion with rates $D_y$and D_x, respectively.

Using these reactions, the ISP dynamics translates into a PP system. The deterministic continuous average description of this ISP model leads to the following ODEs:

$$\frac{\partial x}{\partial t} = \alpha x - \gamma xy \tag{8}$$

$$\frac{\partial y}{\partial t} = \lambda + \nu xy - \sigma y$$

Two possible regimes are expected in the ODE solution of this system: A) a stable zero-pathogen fixed point, where small perturbations decay rapidly to zero, and pathogens never manage to produce a full blown infection; or B) an unstable zero-pathogen fixed point, where the small perturbations converge to the positive fixed point, leading to a coexistence of the host immune system and the pathogen. These regimes do not seem to represent the experimental reality of pathogens growing and disappearing.

In discrete stochastic systems, the population of preys ultimately undergoes extinction. The extinction probability (at a finite time) starting from the positive fixed point decays exponentially with the number of predators and preys in the fixed point [15,18,55,59,65,67,68]. We have studied the transition to the absorbing state, following an escape from the same state [2]. We have shown that starting near the absorbing state, the dynamics of discrete stochastic spatially extended PP models are determined by three factors:

- the extinction probability of a small perturbation from the absorbing state in the discrete stochastic zero-dimensional PP model;
- the diffusion rate;
- the system size.

The interplay between these factors can lead to different dynamical regimes. These regimes are described in the following sections.

In the zero dimensional discrete system, there is a large region in parameter space where the system converges to the absorbing state. Starting from a small perturbation near $(0, y_0)$, the transition to the absorbing state for high values of (x^*, y^*) occurs most probably during the first pass near the zero pathogen state (Fig. 5). Note that if the initial perturbation is too small, there is also a non-negligible probability that the system will directly converge to the absorbing state. We here assume that the initial perturbation is large enough and that this effect is secondary. The probability of moving to the absorbing state at the first pass near zero increases with the time spent at low pathogens value. Let us denote the pathogen extinction probability as $P^{local}_{disapearanc}$. We have previously provided an analytical estimate of $P^{local}_{disapearanc}$ [2]. This convergence probability increases with the value of (x^*, y^*)in the simulations. The disappearance of the pathogens in this system is thus not due to low values of x at the fixed point. It occurs following transient low values on the trajectory to the fixed point. For constant initial conditions, as the values of x^* and y^* increase, the trajectory will pass closer to the y axis (as can be easily seen from a geometrical perspective), and the pathogen disappearance probability in the first pass near zero increases. Equations (8) and their stochastic zero dimensional counterpart (see Methods) were solved numerically for different values of (x^*, y^*). For each value of (x^*, y^*), the fraction of stochastic realizations ending at the absorbing state was computed (Fig. 6). The observed transition to the absorbing state does not result from the low total number of agents in the simulation, but from the large distance between the starting conditions and the positive fixed point.

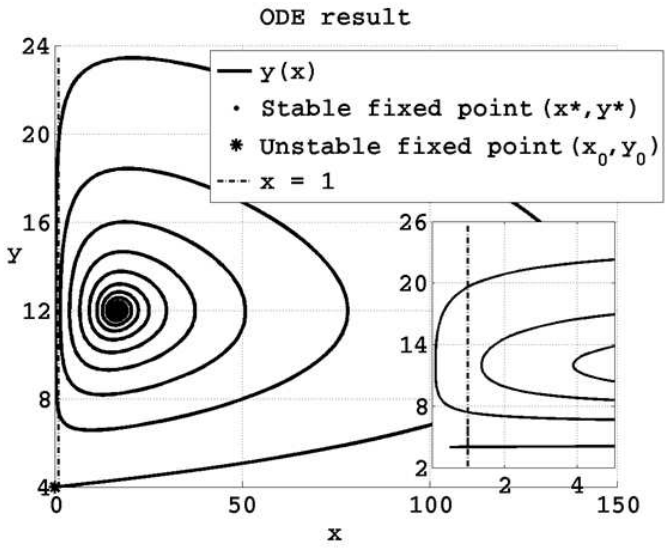

FIGURE 5. **Trajectories of ODE solution of immune system-pathogen dynamics**. The trajectories start from a point near the zero pathogen fixed point and oscillate toward the positive fixed point. At each oscillation, the trajectories get farther away from the y axis. During the first oscillations, the trajectories can stay for a long time in a region where the expected pathogen population is less than 1. In this region there is a high pathogen disappearance probability (inset). The parameters used for these results are: $\alpha = 1.2, \gamma = 0.1, \lambda = 0.4, \nu = 0.004, \sigma = 0.1, D_x = D_y = 0, t = 200$.

Thus, the apparent discrepancy between the observed pathogen rise and extinction and the predictions of the deterministic continuous PP system can be simply explained using the transition of the trajectory very close to the y axis. In other words, at some stage the pathogen number is so low that it shrinks to zero (Fig. 7).

6.2. **Spatially inhomogeneous dynamics.** The effect on $P^{local}_{disapearanc}$ of analyzing the system in space differs for large and small values. If $P^{local}_{disapearanc}$ is low, diffusion stabilizes the positive fixed point (data not shown), as often happens in PP systems [19,29,60]. We are here interested in the opposite regime where $P^{local}_{disapearanc}$ is almost 1.

Assume $P^{local}_{disapearanc}$ is high enough such that the survival probability in one pass near the y axis even in a single spot in the entire system is low. In such a case, the positive fixed point is never obtained in the absence of diffusion. If the diffusion is zero, each region in turn will be absorbed to the zero pathogen state until the entire system will converge to the absorbing state after a single pass near zero. The transition to extinction occurs since regions with no pathogens cannot be colonized

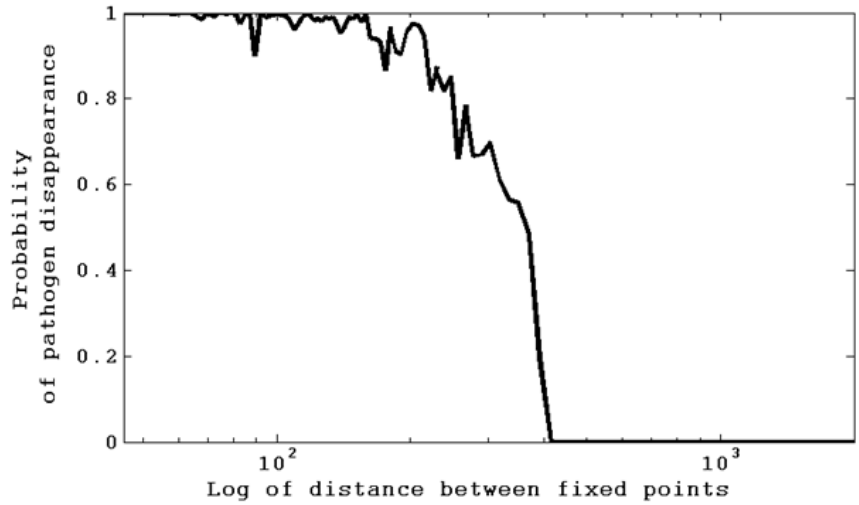

FIGURE 6. **Probability of pathogen disappearance as a function of distance between fixed points**. The pathogen disappearance probability (at the first pass near zero) grows with the distance between the zero pathogen fixed point and the positive fixed point. The parameters used in this figure are: $\alpha = 0.2, \gamma = 0.1, \lambda = 0.4, \sigma = 0.1$, runs from $10^{-5}$to $1.5 \cdot 10^{-3}$. The distance between the fixed points is defined as the Euclidean distance.

by regions where the pathogen concentration is still finite. If the diffusion rate is too high, the system behaves as the mean field and all pathogens die simultaneously as the local pathogen density becomes too low. Thus, if $P^{local}_{disapearanc}$ is high and the diffusion rate is either very low or very high, the pathogen population will disappear (Fig. 8). In intermediate ranges of diffusion rates, colonization can take place and complex dynamics can emerge from the combination of asynchronous pathogen dynamics and the high diffusion rates. Interestingly, within this parameter range, the transition between the two regimes is determined by the system size, and not only by the values of the rate constants.

6.3. **Directed percolation.** At high values of $P^{local}_{disapearanc}$ and intermediate diffusion rates, an interesting invasive regime emerges. At each position independently, the low number of pathogens in the initial condition leads to stochastic variations in the time at which the pathogen population is minimal and to a loss of synchronization. Thus, by the time the pathogen population in a given site is annihilated, neighboring sites may still have a non-zero pathogen population. In such a case, if the diffusion rate is high enough, the pathogen in the neighboring sites can colonize the empty site, once the immune system cells concentration is low enough in the colonized site. Following this invasion, the pathogen population can rise again.

Such a dynamics appears to be similar to a Directed Percolation (DP) model. The fraction of space with a non-zero pathogen population was measured in Monte

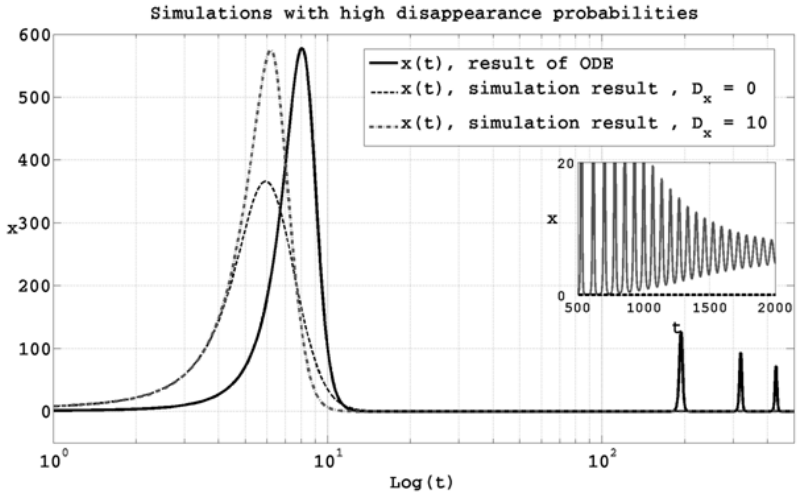

FIGURE 7. **Pathogen dynamics**. Pathogen average population as a function of time for the ODE solution (full line), the $D_x = 0$ stochastic simulation (dashed line) and the $D_x = 10$ stochastic simulation (doted dashed line). Both the low and high diffusion rate simulations converge to the non-stable zero pathogen state in contrast with the mean field ODE. The parameters used for these results are $\alpha = 1.6, \gamma = 0.01, \lambda = 0.6, \nu = 0.001, \sigma = 0.01$.

Carlo simulations of the ISP model in 1, 2 and 3 dimensions for different values of D_x and $P^{local}_{disapearanc}$. We then compared these results to simulations of a DP model with parallel invasion and extinction rates (see Methods). In the DP model, each lattice site was assigned a value of either zero or one. Each lattice site with a value of one could become zero with a probability of $p(dis)$ and invade neighboring sites with a probability of $p(inv)$. The system was initiated with a fully occupied lattice. We ran this simulation for different values of $p(dis)$ and $p(inv)$, and ran in parallel simulations of the full ISP with $p(dis) = P^{local}_{disapearanc}$ and $p(inv) = D_x$ (Fig. 9). After the system converged to its steady state filling fraction, we measured the filling fraction as a function of $p(inv)$. The percolation transition in two and three dimensions is in good agreement with the full ISP dynamics Monte Carlo simulation (Fig. 9 points vs. full line). However, in the one dimensional system, the fit is limited (dashed line). The finite pathogen concentration in this regime results from an amalgam of regions where the pathogen population has vanished and regions re-colonized by the pathogen (data not shown). To summarize, if the diffusion rate is intermediate and $P^{local}_{disapearanc}$ is high, the dynamics can be explained by a simple DP processes that is only determined by $p(dis)$ and $p(inv)$, at least in 2 and 3 dimensions. In one dimension, the precise dynamics of the DP and the full ISP only agrees qualitatively.

6.4. **Wave trains.** In parallel to the DP regime, a different behavior can emerge in the same parameter range. For most simulation trials, the pathogen population follows a DP dynamics. There are, however, rare events, where in one lattice point

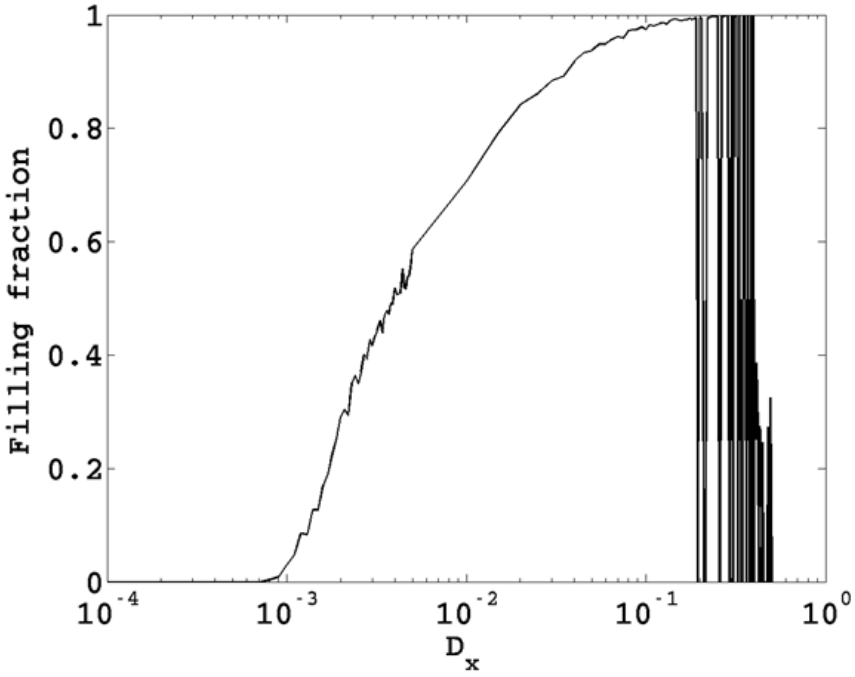

FIGURE 8. **Pathogen filling fraction as a function of diffusion rate**. The stochastic simulations results in 2 dimensions ($d = 2$). The lattice size is 100x100. The parameters used for this figure are :$\alpha = 1.6, \gamma = 0.1, \lambda = 0.4, \nu = 0.004, \sigma = 0.1 D_y = 0.01$. For low and high values of pathogen diffusion rates, the pathogen population goes to extinction. For high values of D_x, there are rare events of population survival. The number of such events decreases as $D_x$grows. Note that the curve is non symmetric. For low diffusion rates, a part of the space is occupied, while for high diffusion rates, either all or nothing is occupied. The filling fraction is defined as the fraction of lattice points with non-zero pathogen values.

the pathogen population does not disappear in multiple passes near zero. In each following pass, the disappearance probability decreases until it is negligible. This point can then convert nearby points to the stable fixed point through the propagation of Fisher waves [20], until the entire space converges to the positive fixed point. The Fisher waves advance with a linear rate, and the filling fraction (the fraction of space with non-zero pathogen population values) grows proportionally to the dimension of the system (see, for example, a quadratic growth in a two dimensional system in Fig. 10). A similar process was observed when computing the dynamics of a predator and a prey occupying a new territory [70, 71], and is called wave trains when the central point is marginally stable.

Since $P^{local}_{disapearanc}$ is finite, there is a chance in any system that has not converged to the zero pathogen state in the entire system to converge locally to the wave trains regime. Following the local convergence, the entire system will eventually attain

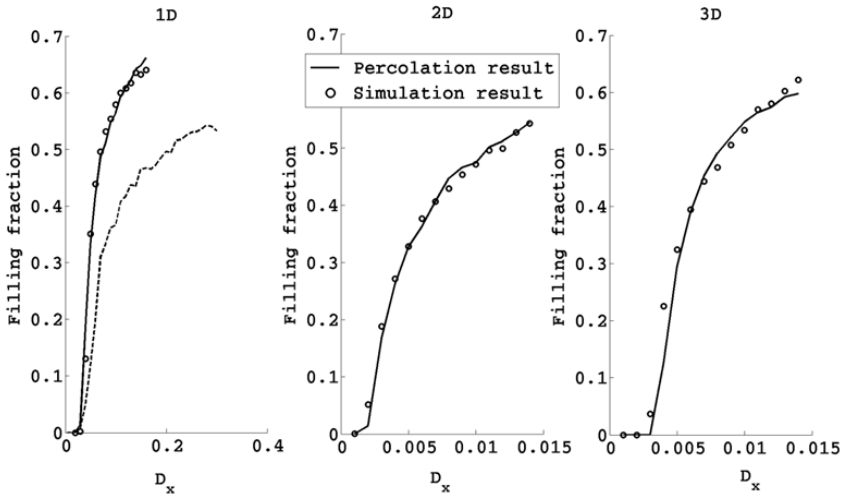

FIGURE 9. **Percolation results and comparison to filling fraction.** The solid line is the percolation transition in the DP model (lattice filling fraction versus $(p(inv))$) which is in good agreement with the full ISP simulation results (scatter plot) (lattice filling fraction versus D_x). For the 2d and 3d systems, the Monte Carlo simulation and DP simulation results coincide for $p(inv) = P^{local}_{disappearance} = 0.35$. In the one dimensional case, the diffusion itself affects $P^{local}_{disappearance}$yielding an effective $P^{local}_{disappearance}$of 0.19. The parameters used in the Monte Carlo simulation are: $\alpha = 1.2, \gamma = 0.2, \lambda = 0.6, \nu = 0.08, \sigma = 0.58$

the positive fixed point value. The only mechanism limiting the transition to the wave trains regime and following it to the stable fixed point is the transition to the absorbing state. The transition probability to the absorbing state in the directed percolation regime is inversely proportional to the exponent of the system size [31]. At any given time, the transition probability to the wave trains regime is linearly proportional to the system size. Thus as the system grows, at finite times, there is a higher probability of transition to the wave trains regime and a lower probability of transition to the absorbing state (Fig. 11). Note that for any system size, the system will always eventually converge to the absorbing state, but the transition rate to extinction may be exponentially small.

To summarize, this system expresses most of the features expressed by the previous ones, mainly the balance between (the pathogen) extinction and its colonization of new regions. An interesting feature made clear by this model is the bell shape relation between the diffusion and the reactant density. At low diffusion value, the bell shape is obtained following the DP phenomena. At high diffusion rate, this is obtained because for high enough diffusion the system converges to the mean field approximation, and collapses back to zero (pathogens).

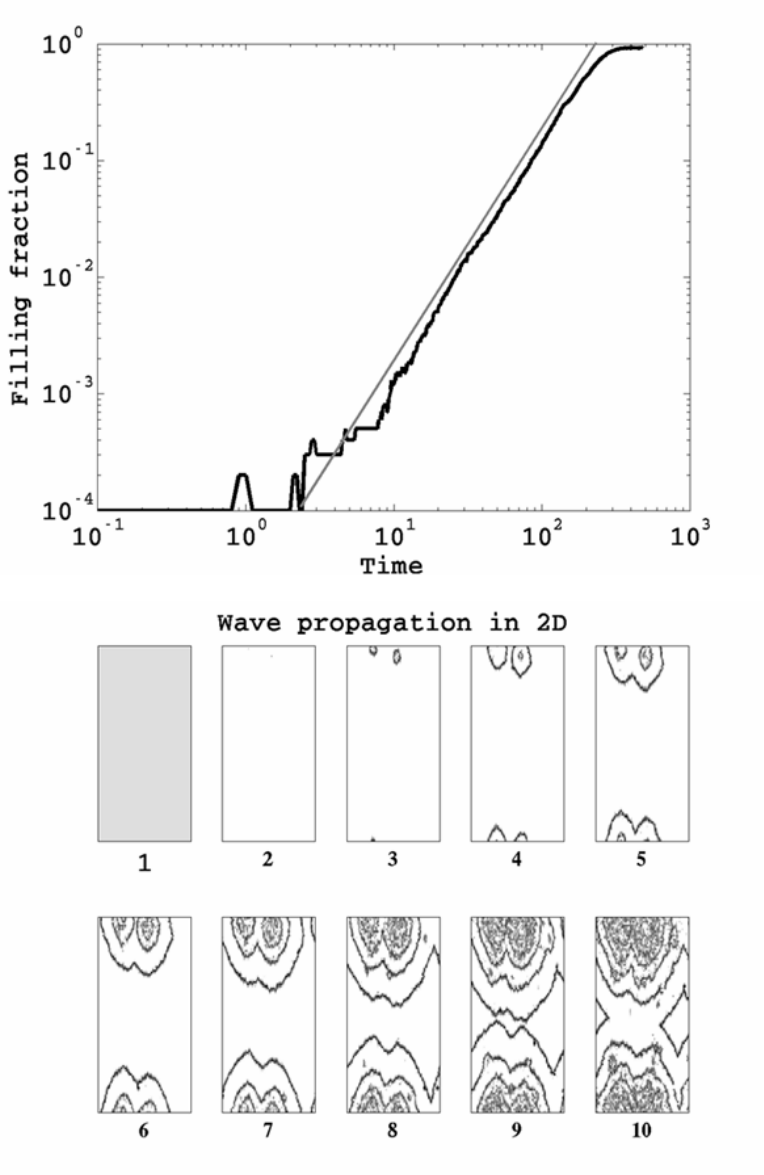

FIGURE 10. **Wave train dynamics**. The upper drawing represents the pathogen filling fraction, which is a quadratic function of time, since the wave front advances at a linear rate in a two dimensional space. The thin gray line is a line representing $y = t^2$. The lower drawing represents the wave creation and propagation in space-time. The first snapshot refers to the uniform filling of the two dimensional space by pathogens. In the second snapshot, the pathogen extinction can be observed in all pixels but two. These two pixels are the source of the following wave that is seen propagating in the next snapshots. The tenth snapshot shows the population survival following the wave filling the 2d space.

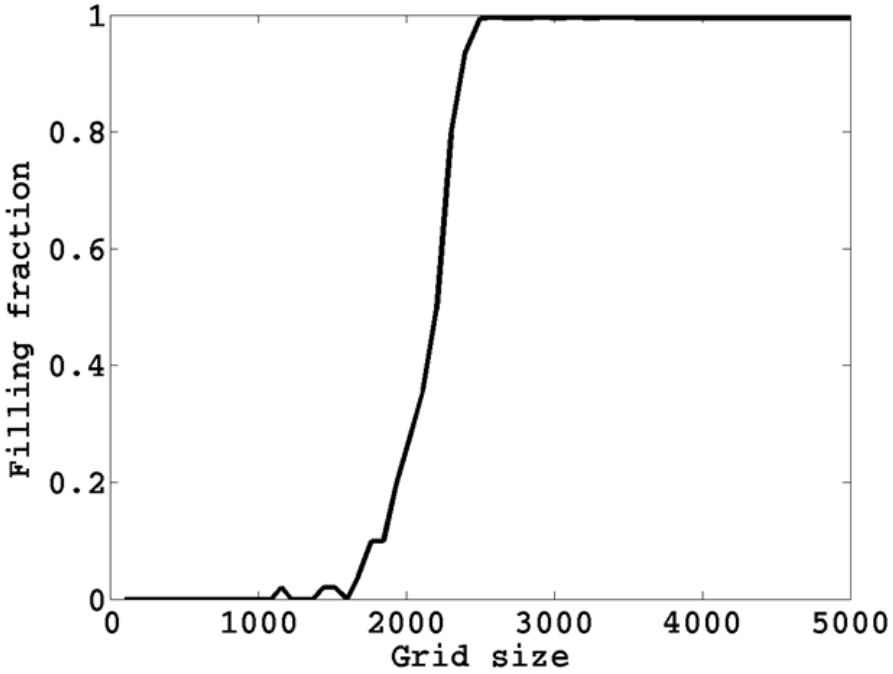

FIGURE 11. **Effect of system size on survival probability**. The ISP simulations were run with the same parameters ($\alpha = 1, 6, \gamma = 0.1, \lambda = 0.4, \nu = 0.004, \sigma = 0.1, D_x = 0.8, D_y = 0.01$) for different two dimensional system sizes, ranging from 10x10 to 150x150. For each system size, 50 realizations were done and the average fraction of non-empty sites was calculated. The filling fraction rises sharply as the system size passes $1/P^{local}_{disappearance}$ until it saturates on 1 in systems significantly larger than that.

7. Model 4 - Resource production.

7.1. **The model - mean filed approximation.** One more model that we discuss is a model of resource production [8]. This model presents the relation between A and B, where A is knowledge and B is capital. The model contains the following reactions:

- $\emptyset \to A$ with a rate of β_A;
- $A \to \emptyset$ with a rate of δ_A;
- $B \to B + A$ with a rate of α_A;
- $A + A \to A$ with a rate of μ;
- $B \to \emptyset$ with a rate of δ_B;
- $A + B \to A + B + B$ with a rate of β_B;
- $B + B \to B$ with a rate of ε.

This model is quite similar to the previous model, where the main difference is the feedback of the B agents on the A agents. The ODE approximation of this model is described in model (9):

$$\frac{dA}{dt} = \beta_A - \delta_A A + \alpha_A B - \mu A^2 \tag{9}$$

$$\frac{dB}{dt} = \beta_B AB - \delta_B B - \varepsilon B^2$$

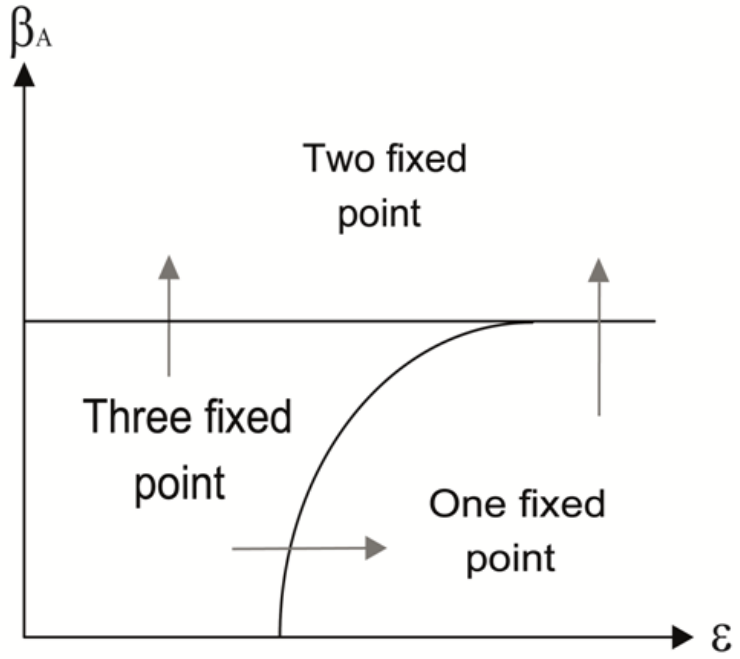

FIGURE 12. **Phase space analysis**. The number of the fixed points as a function of $\beta_A$and ε. The transitions in the system are: three fixed points to one fixed point (by changing ε) , three fixed points to two fixed points and one fixed point to two fixed points (by changing β_A).

The system in Eq.(9) has three possible combinations of fixed points (Figure 12): A single stable fixed point, two fixed points or three fixed points. We focus on the range of the parameters where the system has three fixed points. In this case, this system has two stable fixed points: an absorbing state and a positive fixed point, and one unstable fixed point in between. The values of the fixed points are shown in figure 13 as a function of ε. The solid line is a stable fixed point and the dashed line is an unstable fixed point. Such models classically express a hysteresis mechanism. When starting from a non-zero state, increasing epsilon will lead to a collapse to the absorbing state. However, reducing epsilon back will not return the system to the non-zero state. Such a phenomenon is called hysteresis.

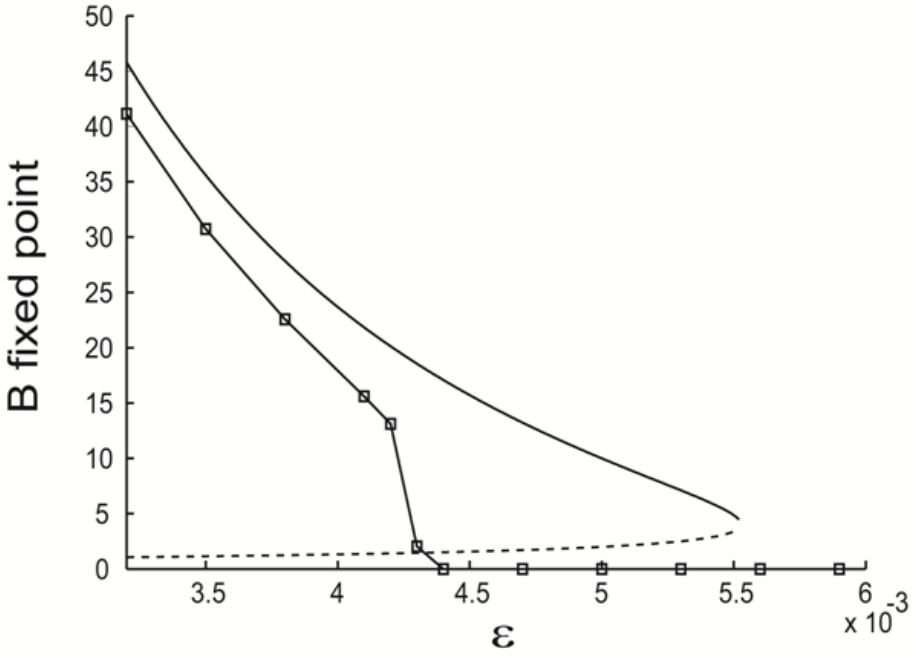

FIGURE 13. The average of B as a function of $\varepsilon$with the parameters: $\delta_A = 0.02, \alpha_A = 0.01, \beta_B = 0.002, \delta_B = 0.01, \mu = 0.00005, \beta_A = 0.005$, with diffusions of A and B at 0.001, initial conditions of $A = 30$, $B = 10$, on a 100x100 lattice. The solid line is the stable fixed points in the ODE. The dashed line is the unstable fixed points in the ODE. The square line is the fixed point in the stochastic system. The results of the stochastic simulation are continuous, and the transitions in the stochastic simulation are shifted compared with the ODE.

7.2. **Stochastic results.** The stochastic simulation stabilizes around a different average from the ODE. Figure 13 shows the mean of B agent density in the stochastic simulation, when ε is varied.

The difference between the hysteresis expected from the ODE model and the stochastic simulation is the result of the non-symmetric transition between the upper fixed point and the absorbing state. In intermediate values of ε, the balance between these two mechanisms produces an inhomogeneous distribution that has a stable average, which is based on a constantly changing spatial distribution of the A and B concentrations (Figure 14).

Figure 15 describes the transition between two stable fixed points in phase space. In a short time, all the values of the B agents in the lattice go to the line that connects between three fixed points. Stochastic fluctuations can then transfer lattice sites from one stable fixed point to the other. This transfer is however non-symmetrical since the low fixed point is an absorbing state. If in a given lattice

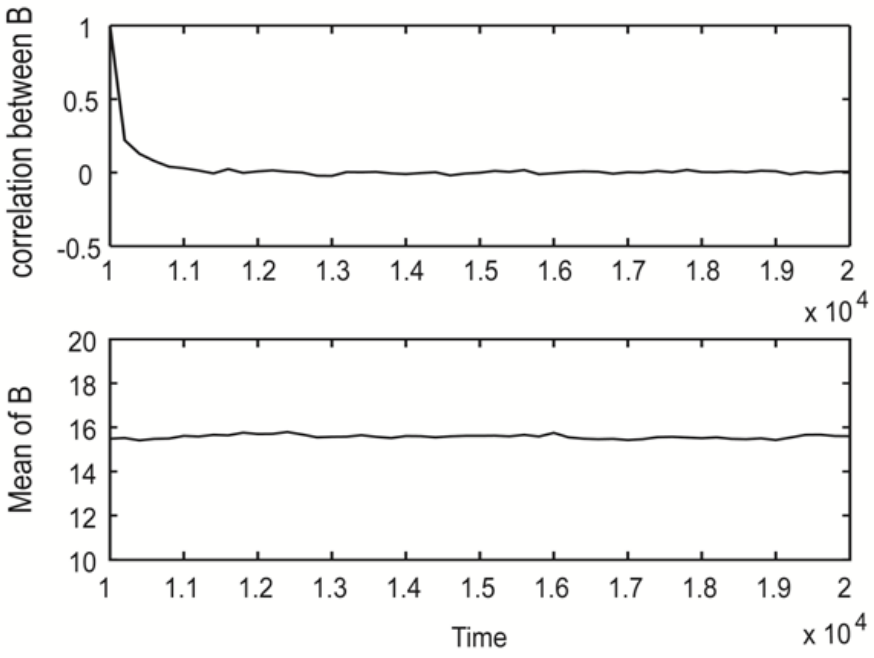

FIGURE 14. **Lack of long term correlations**. Upper drawing. The correlation between the B agents spatial distribution as a function of time, with the following parameters: $\delta_A = 0.002, \alpha_A = 0.005, \beta_B = 0.002, \delta_B = 0.01, \mu_A = 0.01, \mu = 0.00005, \varepsilon = 0.0041$.The lower drawing represents the average B concentration as a function of time. The average B concentration is constant over time, while the correlation goes to zero.

site the B population is extinct (i.e. goes to the low fixed point ($B = 0$)), it cannot leave this point purely through stochastic fluctuations. The only way that this lattice point can be preoccupied by B agents is through diffusion from neighboring lattice sites. In contrast, a lattice site that goes to the high fixed point can jump to the other side of the schematic line through loss to its neighbors induced by diffusions, or following stochastic fluctuation.

When the transition probability from the lower to the higher fixed point is higher than the opposite transition probability, a fisher wave is observer [36], where the high density region converts the low density region at a constant speed (see linear increase in the total A population in Figure 16D and the step by step growth of the region occupied by the higher fixed point in Figure 16B). If on the other hand the transition probability from the upper to the lower fixed point is higher, a natural decay occurs simultaneously over the entire region that is in the upper fixed point, as can be seen in the exponential decrease in the total A population (Figure 16C) and in the local collapse of the A population (Figure 16A).

To summarize, this last system shows all the properties of the previous system, with a bell shape relation between the diffusion rate and the catalyst density (data

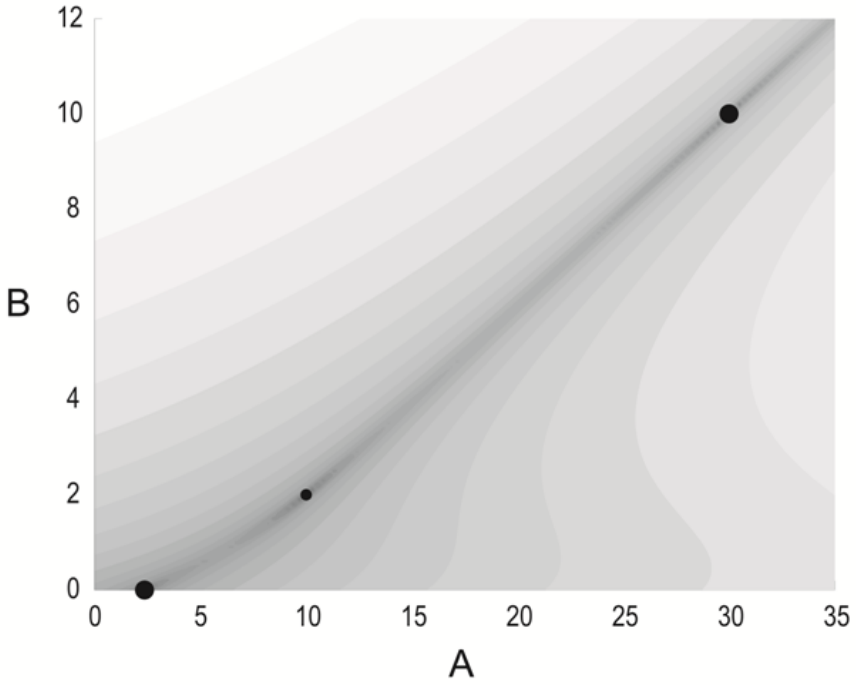

FIGURE 15. **detailed phase space**. Absolute value of gradient as a function of A and B values. Darker colors are closer to zero. One can clearly see that the gradient rises sharply beyond the thin line connecting the three fixed points. The two extreme fixed points are stable (large circles), while the intermediate fixed point (small circle) is not.

not shown), the balance between extinction and invasion and the stark differences between the stochastic and deterministic description of the system.

Thus in many different systems, the balance between the invasion of empty positions in space and the extinction of existing positions determined a diffusion dependent steady state that is not predicted at all by the ODE description of the same systems.

8. **Discussion.** Catalyst induced growth is a frequent phenomenon in many biological and economic systems. These phenomena were previously studied in the context of mean field equations that predict an extinction transition when the average catalyst induced growth rate is equal to the natural death rate. In the generic case of logistic growth or predator prey models, the transition in parameter space is typically assumed to be independent of the diffusion rates. On the other hand, we have previously shown that the stochastic character of the interaction among discrete entities may lead to different behavior as autocatalytic fluctuations may adapt themselves to the fluctuating environment [72]. This phenomenon, and its dependence upon dimensionality (see also [40]) has to do with the features of the localized solutions of the Schrdinger equation for quantum particle in heterogeneous

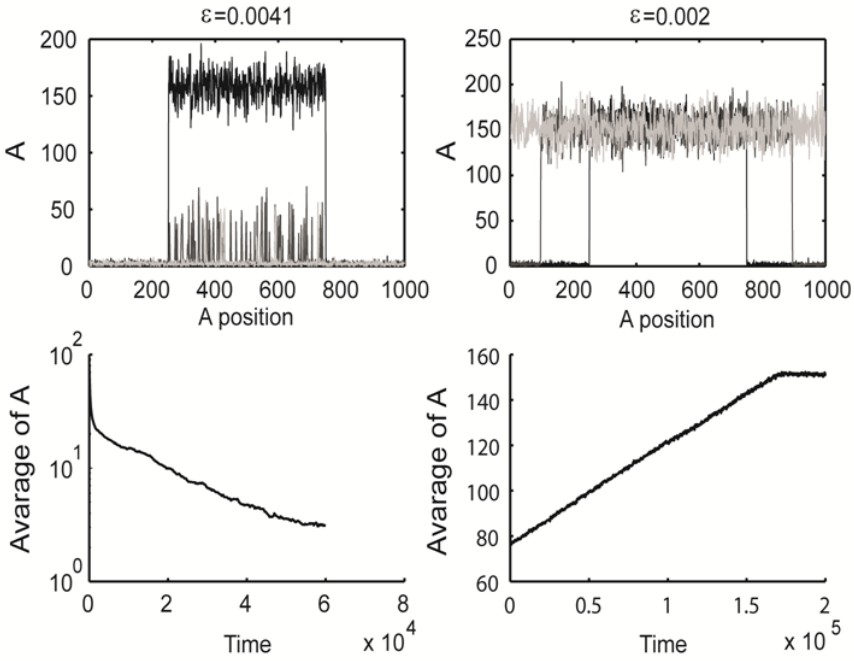

FIGURE 16. **Dynamics following initial condition with half space in the upper state and half in the absorbing state** (The higher figures) Snapshot after 200,000 iterations of the simulation with the parameters $\delta_A = 0.002, \alpha_A = 0.005, \beta_B = 0.002, \delta_B = 0.01, \mu_A = 0.01, \mu = 0.00005, \varepsilon = 0.002$ and $\varepsilon = 0.004$, diffusion of A and B of 0.001, on a 1000x1 lattice. The black line is the initial distribution, the dark gray line is the distribution after 100,000 iterations, and the light gray line is after 200,000 iterations. The lower figures are the averages of A as a function of time. When the system goes to the higher steady state, all the lower points (absorbing state) go to the high steady state in order, and the average of the system goes linearly to the higher steady state ,since the absorbing state goes to higher value through diffusion . When the system goes to the lower steady state, all the lattice sites residing in the high steady state can transfer in parallel to the low steady state, and the average of the system is decreasing approximately exponentially.

environment, very similar to the results obtained in the context of Anderson localization problem [4], and a diffusive motion of the catalysts (i.e., the fact that the random potential of the Anderson-like problem is time dependent) is not strong enough to retain the mean field value.

We have here used a set of models with saturations and predations, all having both an absorbing state and a positive fixed point (in the broad sense of the word, including divergence). The first model studied was a catalyst induced growth model, with a limited catalyst lifespan. The second model studied was a similar model

with limited carrying capacity. The third model included a negative feedback of the reactants on the catalysts producing an extension of the Lotka-Voltera predator prey model. Finally, the fourth model studied contained a positive feedback loop of the reactants on the catalysts producing an economic model where catalysts are actually produced by the reactants.

We have shown that in all these models the dynamics significantly differs from their mean field counterparts. Instead a bell shape response to the diffusion is observed, where at low diffusion rates, the system collapses to the absorbing state locally (and eventually globally). At high values of the diffusion rate, the system synchronizes and converges uniformly to the absorbing state. In between, there is a finite range of diffusion rates where the total reactant population in the system stays finite over exponentially long periods.

Thus two types of transition occur as a function of the diffusion rate: a first transition from low to intermediate diffusion rates, characterized by a transition from extinction to survival, and a second transition from medium to high diffusion rates characterized by the opposite transition.

A simple way to look at the first transition is as a problem of directed percolation with different shapes in the d+1 spatio-temporal dimensions. The mean field description has points like object, while the classical AB model (in the strong coupling limit of low A density) has infinitely growing cones. Accordingly, the directed percolation threshold is in the first case one, and in the second case zero. In the two first models studied, the objects are of finite size in space and time. These colonies have a percolation threshold between zero and one. The difference is in the island shapes, and through it in the percolation threshold. Similarly, in the third model studied, pathogen growth in a host can occur if the pathogen occupies a new niche, before its current niche is destroyed. In the last model studied, resources can collapse following stochastic fluctuations and be reoccupied following diffusion. The balance between these two states is again a DP problem.

Grassberger and Janssen [26,34] proposed that under a set of limiting conditions, many dynamical systems belong to the DP universality class. Only recently the experimental validation of directed percolation was found in (2+1) dimensions [75]. However, altogether, there are very few known two variables systems with a DP behavior. Our work here attempts to provide an example of DP dynamics in a set of more realistic two variable systems.

However, as mentioned above, in contrast with the DP model, these systems have a second opposite transition, where increasing the diffusion rate leads to a collapse of the population. This transition is equivalent to the transition occurring in the AB model, where increasing diffusion leads to a collapsing mean field description of the system.

It thus seems that in many systems, DP describes properly the dynamics at low-medium diffusion rates, while the AB model describes properly the dynamics at medium to high diffusion rates. Realistic systems probably contain a combination of the two. In some parameter regimes, there is no survival region in between, while in others this region (in phase space) is large.

An interesting aspect observed in the studied models, not directly tied to the current analysis is the emergence of Fisher waves. We have also previously studied the relation of PP systems with Fisher waves in the context of HIV dynamics [30]. This was done in the context of a local seeding of the pathogen, and the expansion of the zone where the stable fixed point was attained. One of the currently proposed

models shows that a similar regime can emerge even if the pathogen is seeded uniformly [2]. This is however beyond the scope of the current analysis.

REFERENCES

[1] A. Abbas and A. Lichtman, *Cellular and medical immunology*, Saunders, Philadelphia, (2003), 243–274.

[2] A. Agranovich and Y. Louzoun, *Predator-prey dynamics in a uniform medium lead to directed percolation and wave-train propagation*, Physical Review E, **85** (2012), p. 031911.

[3] A. Agranovich, Y. Louzoun, N. Shnerb and S. Moalem, *Catalyst-induced growth with limited catalyst lifespan and competition*, Journal of Theoretical Biology, **241** (2006), 307–320.

[4] P. W. Anderson, *Absence of diffusion in certain random lattices*, Physical Review, **109** (1958), p. 1492.

[5] R. Arditi and L. R. Ginzburg, *Coupling in predator-prey dynamics: ratio-dependence*, Journal of Theoretical Biology, **139** (1989), 311–326.

[6] K. E. Atkinson, "An Introduction to Numerical Analysis," John Wiley & Sons, 2008.

[7] M. F. Bachmann, B. Odermatt, H. Hengartner and R. M. Zinkernagel, *Induction of long-lived germinal centers associated with persisting antigen after viral infection*, The Journal of Experimental Medicine, **183** (1996), 2259–2269.

[8] H. Behar, N. Shnerb and Y. Louzoun, *Balance between absorbing and positive fixed points in resource consumption models*, Physical Review E, **86** (2012), p. 031146.

[9] A. A. Berryman, *The orgins and evolution of predator-prey theory*, Ecology, (1992), 1530–1535.

[10] C. J. Briggs and M. F. Hoopes, *Stabilizing effects in spatial parasitoid–host and predator–prey models: a review*, Theoretical Population Biology, **65** (2004), 299–315.

[11] S. R. Broadbent and J. M. Hammersley, *Percolation processes i. crystals and mazes*, in "Proceedings of the Cambridge Philosophical Society," **53** 1957, 629–641.

[12] D. H. Busch and E. G. Pamer, *T lymphocyte dynamics during listeria monocytogenes infection*, Immunology Letters, **65** (1999), 93–98.

[13] G. Cai and Y. Lin, *Stochastic analysis of predator–prey type ecosystems*, Ecological Complexity, **4** (2007), 242–249.

[14] A. M. de Roos, E. McCauley and W. G. Wilson, *Pattern formation and the spatial scale of interaction between predators and their prey*, Theoretical Population Biology, **53** (1998), 108–130.

[15] U. Dieckmann and R. Law, *The dynamical theory of coevolution: a derivation from stochastic ecological processes*, Journal of Mathematical Biology, **34** (1996), 579–612.

[16] U. Dieckmann, P. Marrow and R. Law, *Evolutionary cycling in predator-prey interactions: Population dynamics and the red queen*, Journal of Theoretical Biology, **176** (1995), 91–102.

[17] U. Dobramysl and U. C. Tauber, *Spatial variability enhances species fitness in stochastic predator-prey interactions*, Physical Review Letters, **101** (2008), p. 258102.

[18] G. Domokos and I. Scheuring, *Discrete and continuous state population models in a noisy world*, Journal of Theoretical Biology, **227** (2004), 535–545.

[19] Y. Du and S.-B. Hsu, *A diffusive predator–prey model in heterogeneous environment*, Journal of Differential Equations, **203** (2004), 331–364.

[20] R. A. Fisher, *The wave of advance of advantageous genes*, Annals of Human Genetics, **7** (1937), 355–369.

[21] H. Freedman and Y. Takeuchi, *Predator survival versus extinction as a function of dispersal in a predator–prey model with patchy environment*, Applicable Analysis, **31** (1989), 247–266.

[22] H. Freedman and G. Wolkowicz, *Predator-prey systems with group defence: The paradox of enrichment revisited*, Bulletin of Mathematical Biology, **48** (1986), 493–508.

[23] G. Gardiner, "Handbook of Stochastic Processes for Physics," 2002.

[24] G. F. Gause et al., *Experimental analysis of vito volterras mathematical theory of the struggle for existence*, Science, **79** (1934), p. 340.

[25] P. Grassberger, *On phase transitions in schlogls second model*, Zeitschrift fur Physik B Condensed Matter, **47** (1982), 365–374.

[26] P. Grassberger, *Directed percolation in 2+ 1 dimensions*, Journal of Physics A: Mathematical and General, **22** (1989), 3673–3679.

[27] P. Grassberger, H. Chate and G. Rousseau, *Spreading in media with long-time memory*, Physical Review E, **55** (1997), p. 2488.

[28] P. Grassberger, F. Krause and T. von der Twer, *A new type of kinetic critical phenomenon*, Journal of Physics A: Mathematical and General, **17** (1999), p. L105.
[29] A. Hastings, *Global stability of two species systems*, Journal of Mathematical Biology, **5** (1977), 399–403.
[30] U. Hershberg, Y. Louzoun, H. Atlan and S. Solomon, *Hiv time hierarchy: winning the war while, loosing all the battles*, Physica A: Statistical Mechanics and its Applications, **289** (2001), 178–190.
[31] H. Hinrichsen, *Non-equilibrium critical phenomena and phase transitions into absorbing states*, Advances In Physics, **49** (2000), 815–958.
[32] A. R. Ives, B. J. Cardinale and W. E. Snyder, *A synthesis of subdisciplines: Predator–prey interactions, and biodiversity and ecosystem functioning*, Ecology Letters, **8** (2004), 102–116.
[33] C. Janeway and P. Travers, "Immunobiology: The Immune System in Health and Disease," Garland Publ., Inc., New York, NY, 1997.
[34] H.-K. Janssen, *On the nonequilibrium phase transition in reaction-diffusion systems with an absorbing stationary state*, Zeitschrift für Physik B Condensed Matter, **42** (1981), 151–154.
[35] I. Jensen and R. Dickman, *Series analysis of the generalized contact process*, Physica A: Statistical Mechanics and its Applications, **203** (1994), 175–188.
[36] Y. Kan-On, *Fisher wave fronts for the lotka-volterra competition model with diffusion*, Nonlinear Analysis: Theory, Methods & Applications, **28** (1997), 145–164.
[37] C. KELLY, D. CARVALHO and T. TOME, *Self-organized patterns of coexistence out of a predator-prey cellular automaton*, International Journal of Modern Physics C, **17** (2006), 1647–1662.
[38] M. Kenneth, P. Travers and M. Walport, *Janeways immunobiology*, Open ISBN, (2007).
[39] W. Kermack and A. McKendrick, *Contributions to the mathematical theory of epidemics*, Bulletin of Mathematical Biology, **53** (1991), 33–55.
[40] H. Kesten and V. Sidoravicius, *Branching random walk with catalysts*, Electron. J. Probab., **8** (2003), 1–51.
[41] A. Kolmogorov, I. Petrovsky and N. Piskunov, *Etude de lquation de la diffusion avec croissance de la quantit de matiere et son applicationa un probleme biologique*, Mosc. Univ. Bull. Math, **1** (1937), 1–25.
[42] M. Kot, "Elements of Mathematical Ecology," Cambridge University Press, 2001.
[43] R. Law, M. J. Plank, A. James and J. L. Blanchard, *Size-spectra dynamics from stochastic predation and growth of individuals*, Ecology, **90** (2009), 802–811.
[44] P. Leslie and J. Gower, *The properties of a stochastic model for the predator-prey type of interaction between two species*, Biometrika, (1960), 219–234.
[45] A. L. Lin, B. A. Mann, G. Torres-Oviedo, B. Lincoln, J. Käs and H. L. Swinney, *Localization and extinction of bacterial populations under inhomogeneous growth conditions*, Biophysical Journal, **87** (2004), 75–80.
[46] A. J. Lotka, *Undamped oscillations derived from the law of mass action*, Journal of the American Chemical Society, **42** (1920), 1595–1599.
[47] A. J. Lotka, *Contribution to the energetics of evolution*, Proceedings of the National Academy of Sciences of the United States of America, **8** (1922), p. 147.
[48] A. J. Lotka, "Elements of Physical Biology," Williams & Wilkins Baltimore, 1925.
[49] Y. Louzoun, S. Solomon, H. Atlan and I. Cohen, *The emergence of spatial complexity in the immune system*, Physica A, **297** (2001), 242–252.
[50] Y. Louzoun, S. Solomon, H. Atlan, I. Cohen, et al., *Microscopic discrete proliferating components cause the self-organized emergence of macroscopic adaptive features in biological systems*, preprint, `arXiv:nlin/0006043`, (2000).
[51] Y. Louzoun, S. Solomon, H. Atlan and I. R. Cohen, *Modeling complexity in biology*, Physica A: Statistical Mechanics and its Applications, **297** (2001), 242–252.
[52] Y. Louzoun, S. Solomon, H. Atlan and I. R. Cohen, *Proliferation and competition in discrete biological systems*, Bulletin of Mathematical Biology, **65** (2003), 375–396.
[53] Y. Louzoun, S. Solomon, J. Goldenberg and D. Mazursky, *World-size global markets lead to economic instability*, Artificial Life, **9** (2003), 357–370.
[54] T. R. Malthus, *An essay on the principle of population, as it affects the future improvement of society: With remarks on the speculations of mr. Godwin, mr. Condorcet, and other writers*, New York: Penguin, (1798).
[55] M. Mobilia, I. T. Georgiev and U. C. Täuber, *Fluctuations and correlations in lattice models for predator-prey interaction*, Physical Review E, **73** (2006), p. 040903.

[56] M. Mobilia, I. T. Georgiev and U. C. Täuber, *Spatial stochastic predator-prey models*, Stochastic models in biological sciences, 253–257, Banach Center Publ., 80, Polish Acad. Sci. Inst. Math., Warsaw, 2008.
[57] M. Murray, "Jd Mathematical Biology," 1989.
[58] D. R. Nelson and N. M. Shnerb, *Non-hermitian localization and population biology*, Physical Review E, **58** (1998), 1383–1403.
[59] M. G. Neubert and M. Kot, *The subcritical collapse of predator populations in discrete-time predator-prey models*, Mathematical Biosciences, **110** (1992), 45–66.
[60] M. G. Neubert, M. Kot and M. A. Lewis, *Dispersal and pattern formation in a discrete-time predator-prey model*, Theoretical Population Biology, **48** (1995), 7–43.
[61] A. J. Nicholson and V. A. Bailey, *The balance of animal populations.*, in "Proceedings of the Zoological Society of London," **105**, Wiley Online Library, (1935), 551–598.
[62] A. Okubo, "Diffusion and Ecological Problems: Mathematical Models," Springer, New York, 1980, xiii+254.
[63] M. Rambeaud, R. Almeida, G. Pighetti and S. Oliver, *Dynamics of leukocytes and cytokines during experimentally induced streptococcus uberis mastitis*, Veterinary Immunology and Immunopathology, **96** (2003), 193–205.
[64] L. Reichl, "A Modern Course in Statistical Physics," Wiley, New York, 1998.
[65] B. A. Reid, U. C. Tauber and J. C. Brunson, *Reaction-controlled diffusion: Monte Carlo simulations*, Physical Review E, **68** (2003), p. 046121.
[66] M. L. Rosenzweig et al., *Paradox of enrichment: destabilization of exploitation ecosystems in ecological time*, Science, **171** (1971), 385–387.
[67] A. Rozenfeld, C. Tessone,E. Albano, and H. Wio, *On the influence of noise on the critical and oscillatory behavior of a predator–prey model: coherent stochastic resonance at the proper frequency of the system*, Physics Letters A, **280** (2001), 45–52.
[68] R. Rudnicki and K. Pichor, *Influence of stochastic perturbation on prey-predator systems*, Mathematical Biosciences, **206** (2007), 108–119.
[69] M. Schaeffer, S.-J. Han, T. Chtanova, G. G. van Dooren, P. Herzmark, Y. Chen, B. Roysam, B. Striepen and E. A. Robey, *Dynamic imaging of t cell-parasite interactions in the brains of mice chronically infected with toxoplasma gondii*, The Journal of Immunology, **182** (2009), 6379–6393.
[70] J. A. Sherratt, *Invading wave fronts and their oscillatory wakes are linked by a modulated travelling phase resetting wave*, Physica D: Nonlinear Phenomena, **117** (1998), 145–166.
[71] J. A. Sherratt and M. J. Smith, *Periodic travelling waves in cyclic populations: field studies and reaction–diffusion models*, Journal of the Royal Society Interface, **5** (2008), 483–505.
[72] N. Shnerb, E. Bettelheim, Y. Louzoun, O. Agam and S. Solomon, *Adaptation of autocatalytic fluctuations to diffusive noise*, Physical Review E, **63** (2001), p. 021103.
[73] N. M. Shnerb, Y. Louzoun, E. Bettelheim and S. Solomon, *The importance of being discrete: Life always wins on the surface*, Proceedings of the National Academy of Sciences, **97** (2000), 10322–10324.
[74] J. Skellam, *Random dispersal in theoretical populations*, Biometrika, (1951), 196–218.
[75] K. A. Takeuchi, M. Kuroda, H. Chate and M. Sano, *Directed percolation criticality in turbulent liquid crystals*, Physical review letters, **99** (2007), 234503.
[76] P.-F. Verhulst, *Recherches mathematiques sur la loi daccroissement de la population*, Memoires de lAcademie Royale des Sciences et des Belles-Lettres de Bruxelles, **18** (1845), 1–45.
[77] V. Volterra, *Variazioni e fluttuazioni del numero d'individui in specie animali conviventi*, Mem. Acad, Lincei 22, 31, 113 (1926).
[78] M. J. Washenberger, M. Mobilia and U. C. Tauber, *Influence of local carrying capacity restrictions on stochastic predator–prey models*, Journal of Physics: Condensed Matter, **19** (2007), 065139.
[79] G. Yaari, S. Solomon, M. Schiffer and N. M. Shnerb, *Local enrichment and its nonlocal consequences for victim–exploiter metapopulations*, Physica D: Nonlinear Phenomena, **237** (2008), 2553–2562.

Received July 02, 2012; Accepted September 13, 2012.

E-mail address: hilla.behar2@gmail.com
E-mail address: alexana77@gmail.com
E-mail address: louzouy@math.biu.ac.il